

Supporting Information

Synthesis of stable near-infrared emitting HgTe/CdS core/shell nanocrystals using dihydrolipoic acid as stabilizer

Wen-Hao Zhang¹, Jing Yang^{1,2} and Jun-Sheng Yu^{1*}

1. State Key laboratory of Analytical Chemistry for life Science, School of Chemistry and Chemical Engineering, Nanjing University, Nanjing 210093, P. R. China.

2. School of Pharmacy, Nanjing Medical University, Nanjing 210029, P. R. China

Synthesis of DHLA-capped HgTe NCs

In a typical synthesis, firstly, Te powder (40 mg) was reduced by NaBH₄ (80 mg) under N₂ atmosphere in solution of water/alcohol (1/2, v/v) at 60°C for about 20 min. After black Te powder was completely reduced, 3 mL H₂SO₄ (0.5 mol/L) was introduced to generate H₂Te gas that was absorbed in turn with 2 mL NaOH (0.1 mol/L) aqueous solution to obtain NaHTe solution (0.2 mol). Thus, the fresh NaHTe solution was pressed into an oxygen-free 2.5 mL Hg²⁺ (0.2 mol/L) solutions in the presence of 2 mL DHLA (0.5 mol/L) at pH 11.4 by a N₂ flow. Immediately, the colorless solution changed to golden yellow, indicating the formation of HgTe NCs. The resulting solution was heated at 75°C to obtain HgTe NCs with different sizes.

Fluorescence quantum yields measurements of HgTe/CdS core/shell NCs

Fluorescence QYs of HgTe/CdS NCs were measured according to the similar method described in CdTe NCs.^[1,2] In detail, with aim to reduce the measurement error in different luminescence bands, IR-125 (the NIR dye) was chose as the reference standard to calculate fluorescence QYs. During the experiment, the maximum absorption wavelength of IR-125 (765 nm) was set as the excitation wavelength to measure PL QYs of IR-125. The HgTe/CdS NCs had a broad excited spectrum, and a higher fluorescence QY was obtained when 467 nm was used to determine the PL NCs. The absorbance of the 765 nm of the dye and 467 nm of the HgTe/CdS NCs were below 0.1 in order to avoid any significant reabsorption.

In order to reduce the measurement error as much as possible, six respective different concentration solutions of IR-125 (DMSO, quantum yield ~13%^[3]) and HgTe/CdS colloidal solutions were used in the measurements. The areas of integrated fluorescence intensity vs.

absorbance were plotted. The plots yielded two straight lines. The gradients of the straight lines were then used to determine the PLQY according to the following equation:

$$Q_x = Q_s \left(\frac{M_x}{M_s} \right) \left(\frac{\eta_x}{\eta_s} \right)^2$$

where η is the average refractive index of the solvent, M is the gradient of straight line, Q is quantum yield and the subscripts x and s refer to the test samples and reference solutions, respectively. In addition, all optical measurements were performed at room temperature under ambient conditions and ultrapure water was used throughout the whole process.

NIR fluorescence imaging system

A NL-FC-2.0-763 laser ($\lambda=765.9$ nm) was coupled with a NIR optical fiber bundle and defocused to provide a broad shining spot on the surface of the mouse. A high sensitive NIR CCD camera (Princeton, America) was positioned 10 cm above the mouse. An 800 nm long pass filter (Chroma, Rockingham, VT) was put ahead of the CCD to block the excitation and ambient light, and thus to capture the emitted fluorescence from the mouse. The imaging capture was controlled by the matched software and all of operations were performed under dark surroundings at room temperature. The mouse was anesthetized with an intraperitoneal injection of 150 μ L ethyl carbamate (20 mg/mL) and then immobilized in a plate for NIR fluorescence imaging. Furthermore, we got the permission to perform living animal experiments at China pharmaceutical university.

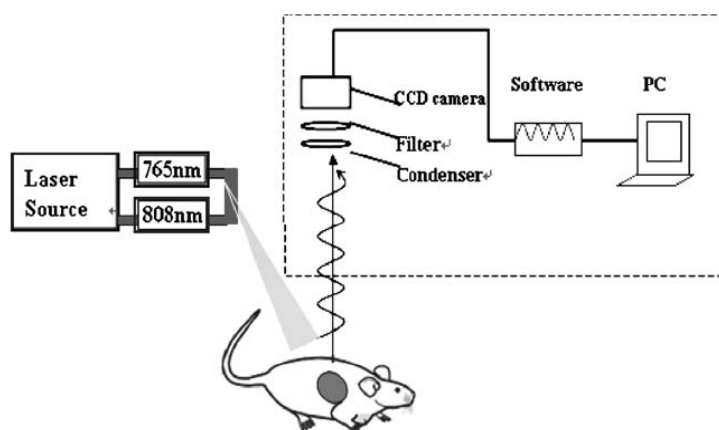


Fig. S1 Schematic diagram of NIR imaging system for fluorescence images.

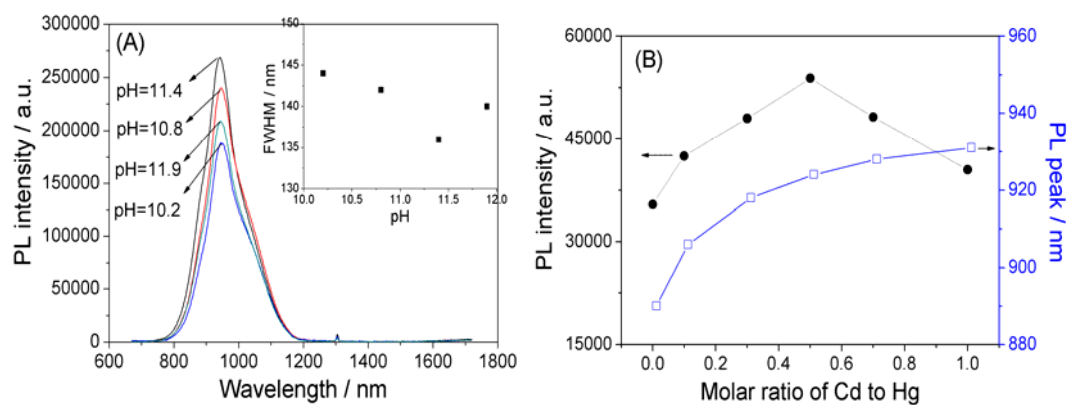


Fig. S2 (A) Influence of pH values on the PL spectra of the HgTe/CdS NCs. Insert: FWHM at different pH values. (B) Influence of Cd/Hg molar ratio on the PL intensity and peak positions of HgTe/CdS NCs.

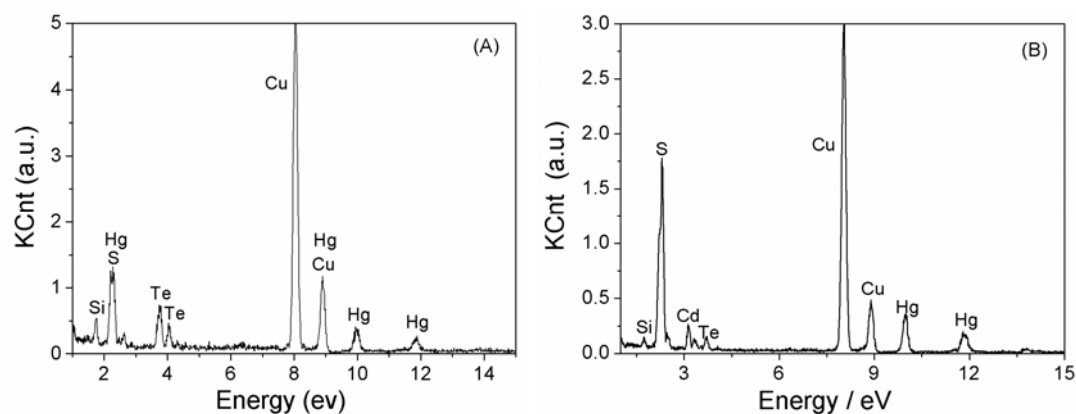


Fig. S3 EDX spectra of DHLA-capped HgTe (A) and HgTe/CdS (B) NCs.

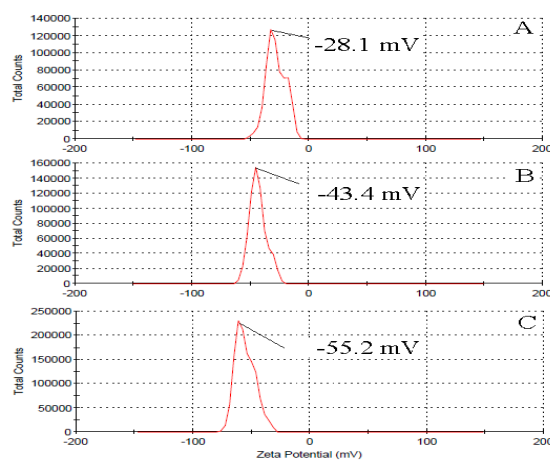


Fig. S4 Zeta potential distribution of TG-capped HgTe (A), DHLA-capped HgTe (B) and DHLA-capped HgTe/CdS NCs (C).

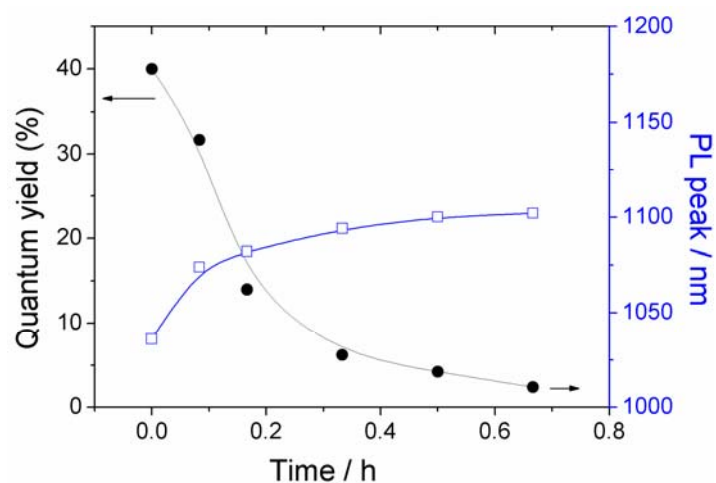


Fig. S5 Time evolution of PL peaks and QYs of TG-capped HgTe NCs with different time when heated at 75°C.

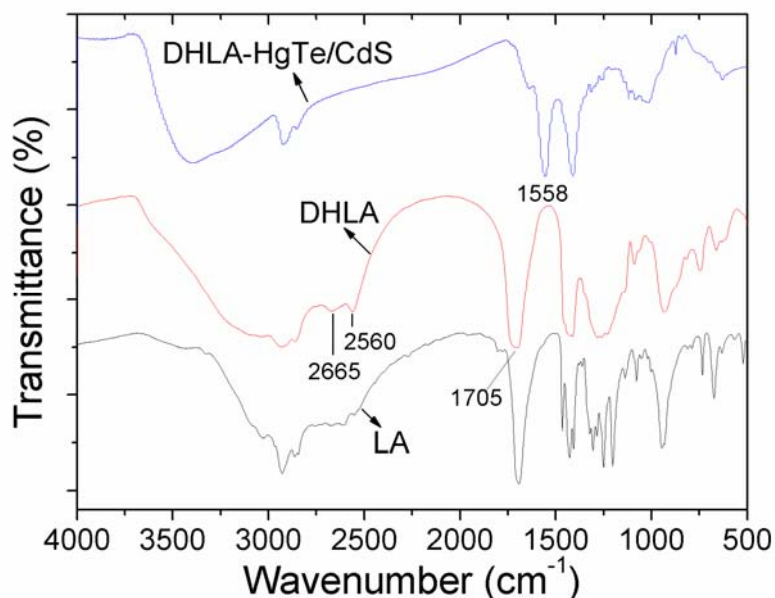


Fig. S6 FT-IR spectra of Lipoic acid (bottom), DHLA (middle) and DHLA –capped HgTe/CdS NCs (top), respectively.

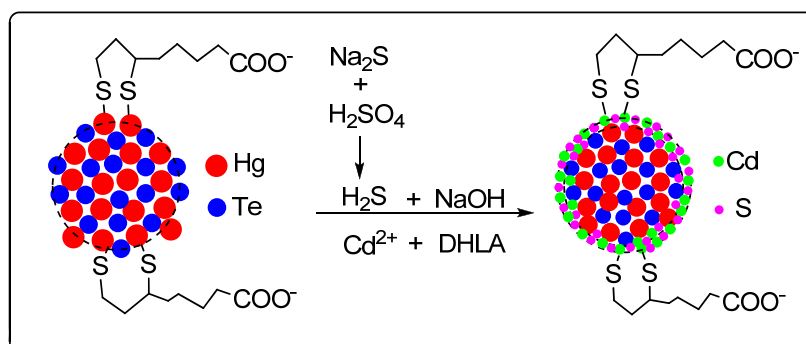


Fig. S7 Schematic diagram of the possible growth process of DHLA-capped HgTe/CdS core/shell NCs.

References:

1. L. Li, H. Qian and J. Ren, *Chem. Commun.*, 2005, 528-530.
2. Y. He, L.-M. Sai, H.-T. Lu, M. Hu, W.-Y. Lai, Q.-L. Fan, L.-H. Wang and W. Huang, *Chem. Mater.*, 2007, **19**, 359-365.
3. R. C. Benson and H. A. Kues, *J. Chem. Eng. Data*, 1977, **22**, 379-383.